

Conductivity of oriented polyacetylene doped by alkali metals: Time, temperature, and pressure dependence

M. R. Andersson

*Institute for Polymers and Organic Solids, University of California at Santa Barbara, Santa Barbara, California 93106
and Department of Organic Chemistry, Chalmers University of Technology, S-41296 Göteborg, Sweden*

K. Väkiparta,* M. Reghu, Y. Cao, and D. Moses

*Institute for Polymers and Organic Solids, University of California at Santa Barbara, Santa Barbara, California 93106
(Received 19 October 1992)*

We report the time, temperature, and pressure dependence of conductivity of oriented polyacetylene doped by alkali metals. The *in situ* conductivity data show that the doping process, by intercalation, is dependent on the size and structural ordering of the ions in the polyacetylene matrix. Steplike features in the *in situ* conductivity measurements show the presence of doping-induced staging transitions. The temperature dependence of conductivity follows a power law, indicating that the system is at the critical regime of the metal-insulator transition, for which the Fermi level is near the mobility edge. We find a weaker temperature dependence for potassium-doped polyacetylene as compared to sodium-doped polyacetylene. The increase of conductivity at high pressures as well as its weaker temperature dependence shows the important role of the interchain interactions for improving the conductivity of alkali-metal-doped oriented polyacetylene.

INTRODUCTION

The conductivity of doped oriented polyacetylene $(\text{CH})_x$, is of magnitude on the order of 10^4 S/cm.¹ The temperature-independent Pauli susceptibility indicates the presence of metallic states in doped $(\text{CH})_x$.² Nevertheless, the typical negative temperature coefficient of resistivity of doped- $(\text{CH})_x$ exhibits nonmetallic behavior, which may arise due to inhomogeneous doping, disorder, carriers localized at defects, etc.¹ These features suggest the important role of interchain-hopping transport, which may be the "bottleneck" for the transport mechanism in this quasi-one-dimensional system. Previous studies of the effect of pressure on the optical properties of undoped $(\text{CH})_x$ have indicated that high hydrostatic pressure redshifts the absorption edge.³ The effect of pressure on the band structure of $(\text{CH})_x$ arises from the decrease of the interchain distance and the increase of the overlap integrals of wave functions.³ In this paper we examine the effect of hydrostatic pressure on the conductivity of doped, oriented $(\text{CH})_x$.

Since the alkali-metal ions are smaller than many *p*-type dopants, a smaller separation of chains may occur during the intercalation process of the counterions into the polymeric matrix. Nevertheless, the maximum conductivity⁴ of *n*-type doped $(\text{CH})_x$ is lower than that of *p*-doped $(\text{CH})_x$,^{5,6} a fact which may arise from the higher chemical reactivity of the *n*-type dopants, resulting in breakdown of the conjugation length. This observation has motivated us to make a systematic study of *in situ* conductivity of $(\text{CH})_x$ doped by different alkali metals, and of the dependence of the conductivity on the doping time, pressure, and temperature. Indeed we find that pressure increases the conductivity and weakens its temperature dependence; in addition, the dependence of the

transport properties on the alkali-metal dopant also indicates the importance of interchain hopping for the transport properties.

EXPERIMENTAL DETAILS

Oriented $(\text{CH})_x$ films were prepared according to the nonsolvent method described by Akagi *et al.*⁷ The samples were further oriented by stretching the films by a factor of 7–10.⁸ Samples of thickness that ranges between 7 and 25 μm were doped in a tetrahydrofuran (THF) solution of alkali-metal naphthalides. The doping solutions were prepared in a dry box by adding excess amount of alkali metal into THF solution of naphthalene, and then allowing it to react for a minimum of 3 h to ensure complete reaction with naphthalene.^{9,10}

Generally, rather few published transport data of alkali-metal-doped $(\text{CH})_x$ are available, probably due to the extreme sensitivity of the *n*-type doped materials to conducting paints, air, impurities, etc. as compared to *p*-type doped $(\text{CH})_x$.^{4,11} Since conducting adhesives dissolve in THF, we prefer to use pressure contacts. We developed a miniature sample holder consisting of spring-loaded contacts that retains good electrical contact under hydrostatic pressure and low-temperature conditions. This miniature pressure-contact assembly consists of two ceramic blocks held together by four platinum (Pt) leads with a pair of heat-treated beryllium-copper spring foils between them, as shown in Fig. 1(a). One side of the sample is exposed to the doping solution so that fast and uniform doping can be achieved. Yet, at low temperatures the contacts occasionally open due to the differential thermal contraction of various parts of the pressure-contact assembly. We eliminated this problem by thinly coating the (Pt) wires with gold paint at the contact region in order to obtain better adhesion with the

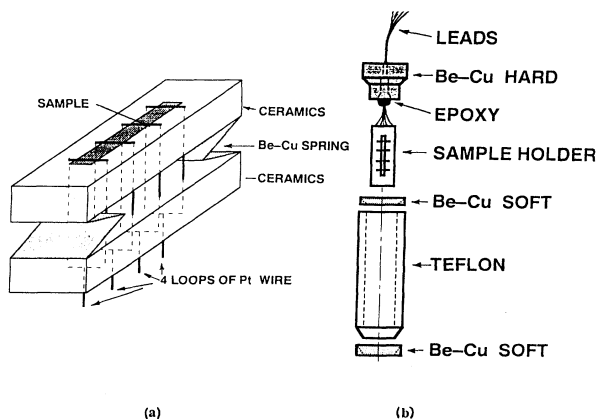


FIG. 1. (a) Spring-loaded pressure-contact assembly; (b) pressure-cell assembly including the Teflon cell, BeCu cap and feedthrough, and soft BeCu sealing rings.

sample. This paint, confined between the wires and sample, apparently does not dissolve into the solution.

The *in situ* room-temperature conductivity experiments were prepared in a glove box where the sample and the doping solution were placed in a sealed glass container, which is equipped with a Pt wire feedthrough, so that it could be taken out of the dry box for dc-conductivity measurements in atmospheric conditions; the data accumulation of the time-dependent conductivity was obtained, every 30–600 s, by a computer-controlled measuring system. In a separate measurement, we found the ionic conductivity of the solutions negligible (10^{-5} S/cm) compared to the electronic conductivity (about 4000 S/cm) of the samples. We have also used highly pure hexane as pressure medium and found the experimental results to be identical.

The samples were pressurized in a self-clamped high-pressure apparatus made of beryllium-copper.^{12–14} The high-pressure Teflon cell assembly is shown in Fig. 1(b). Pt wires were soldered to insulated copper wires that are taken out through the feedthrough located in the beryllium-copper cap of the Teflon cell. The feedthrough is sealed with Stycast 2850 FT epoxy. The polyimide insulation of copper wires is found to be resistant to the THF solution, which is essential for avoiding shorting between the electrical leads. The doping solution itself, or high-purity hexane, is used as the pressure-transmitting medium in order to avoid contamination of the doped polymer during the experiment. The samples prepared for high-pressure studies were doped inside a glove box by immersion into potassium naphthalide (5 mM) for 8–12 h. The Teflon cell was first “preconditioned” by allowing it to react with the dopant solution for 10–15 min in order to avoid contamination during the measuring process and reduction of the dopant concentration. The conductivity of the samples in the pressure cell is quite stable even after it is removed from the dry box; a decrease of less than 10% occurred after 24 h. The pressure cell is clamped at room temperature and then cooled down to 1.2 K in a helium cryostat.

RESULTS AND DISCUSSION

A. *In situ* conductivity

Recent improvement of the quality of pristine $(\text{CH})_x$ films has increased remarkably the maximum conductivities of K-, Rb-, and Cs-doped polymer.^{4,15,16} A comparison of *in situ* conductivities, as a function of doping time, for various alkali-metal dopants (solution concentration of 10 mM) is shown in Fig. 2(a). All the time-dependent conductivity measurements were carried out at ambient pressure. Generally, upon doping, the conductivity rapidly increases, reaches a maximum, and thereafter decreases slightly. Before reaching the maximum, distinct steps consisting of small plateaus and abrupt jumps of the conductivity are clearly evident as shown in the inset of Fig. 2(a). These steps were observed in electrochemical K-doping experiments and correlated by structural determination with distinct staging transitions.^{17,18} The staging transitions in alkali-doped polyacetylene $[(\text{C}_n\text{H}_n)_m\text{K}]$ is defined by m $(\text{CH})_x$ chains per channel of alkali ion in the (a,b) plane and n (CH) units per alkali ion along the c direction. The stage-2 (in doping concentration of 6.2%) to stage-1 (in the doping concentration 6.2–15%) transition is achieved when m decreases from 4 to 2; associated with this staging transition in K-doped $(\text{CH})_x$, the crystalline coherence length increases from 25 to 65 Å.¹⁸ In particular, for K-doped $(\text{CH})_x$ it was found that the peak in the conductivity corresponds to a crossing from a stage-2 to a stage-1 configuration. The slight decline in the conductivity thereafter stems from the completion of the stage-1 configuration, as the channels of potassium ions are filled.

It is interesting to note that although the highest conductivity of Na-doped stretched-oriented sample reached is on the order of that reached by doping with K, Rb, and Cs, its conductivity decays very rapidly to a rather low value (~ 200 S/cm), while for the other alkali metals the conductivity levels off at values above ~ 1500 S/cm and remains stable for a long time, as shown in Fig. 2(b). The distinct behavior of Na-doped $(\text{CH})_x$ apparently stems from the enhanced structural disorder¹⁹ at the higher doping levels, whereas the doping-induced disorder for the larger ions (Cs, Rb, K) is not significant. The lower maximum of conductivity observed in Cs-doped $(\text{CH})_x$ can be understood to arise from the larger interchain distance required to accommodate the larger Cs ions.

The extent of doping-induced structural disorder is apparently strongly dependent on the doping rate, as is clearly revealed in *in situ* studies of the conductivity with different concentrations of doping solution. The rate of increase of the conductivity is higher for the more concentrated solution (10 mM), but the magnitudes of both the maximum and the final conductivities are considerably lower than those obtained by doping with a less concentrated solution (5 mM) [see the inset of Fig. 2(b)]. In addition, for doping with the more concentrated solution, the distinct steps in the conductivity-versus-time data almost disappeared. This is consistent with the increase of structural disorder upon rapid doping that destroys the well-defined staging transitions. Thus, a fast rate of dop-

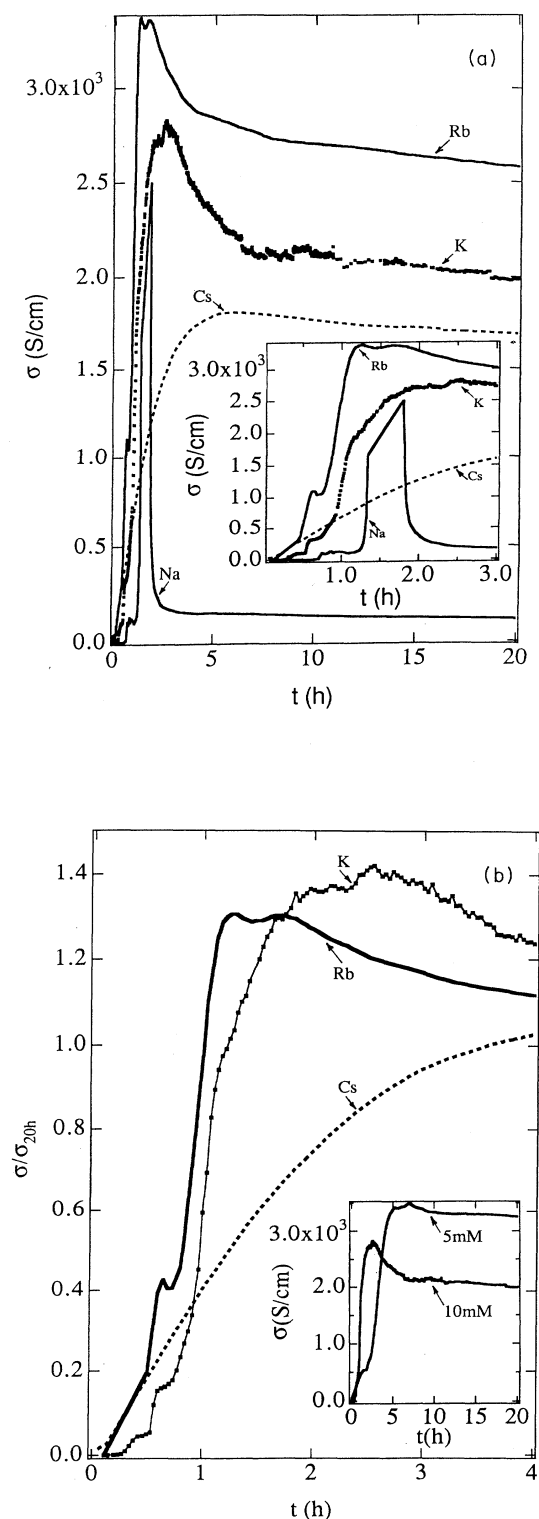


FIG. 2. (a) *In situ* conductivity vs doping time for Na, K, Rb, and Cs; inset shows in more detail the steps in the conductivity at the onset of intercalation. (b) Time dependence of conductivity, normalized by the values after 20 h, for K, Rb, and Cs at ambient pressure; inset shows the conductivity vs time for K-doped $(\text{CH})_x$ for two concentrations.

ing that can be achieved by either increasing the doping solution concentration or employing dopants with smaller ionic size are associated with enhanced disorder. This observation may also explain the higher conductivity of Rb-doped $(\text{CH})_x$ as compared to that of K-doped $(\text{CH})_x$ in our experiments (another possibility is that the co-insertion of THF molecules along with the dopant ions is more probable for K doping).^{10,19}

Thus, upon doping, two competing mechanisms prevail in our *in situ* experiments: increase of the conductivity due to increase of the carrier density and a simultaneous structural disorder. For any particular dopant, the eventual conductivity depends on which mechanism is dominant. Apparently, doping-induced structural disorder is not the only factor that determine the magnitude of the conductivity. Previous¹³ *in situ* conductivity measurements of electrochemically doped K-doped $(\text{CH})_x$ indicate that during intercalation the system undergoes staging transitions at which the electronic properties change drastically; for instance, at the transition from an undoped to a stage-2 structure the conductivity increases by 10 orders of magnitude and the ESR linewidth is reduced by a factor of 40. However, at higher doping levels when a transition from stage-2 to stage-1 takes place, a reduction in conductivity¹⁷ and an increase in ESR linewidth²⁰ (by a factor of 1.7 and 1.4, respectively) occur. A similar decrease in conductivity at the higher doping concentration has been observed in AsF_5 intercalation graphite compound at the transition from stage 2 to stage 1.²¹ Thus, in addition to the structural disorder, the decrease in conductivity at the higher doping levels for K, Rb, and Cs may be associated with such staging transitions.

An additional important factor affecting the conductivity is the intrachain and interchain coupling in the intercalation compound. For instance, the maximum possible doping levels for K and Na are 18% and 11%, respectively.²² Therefore, in K-doped $(\text{CH})_x$, the separation between adjacent solitons, which is much smaller than that in Na-doped $(\text{CH})_x$, results in higher intrinsic conductivity.²³ Other factors that may affect the conductivity are the increase in disorder along the columns of alkali counterions and the commensurate pinning of the charge carriers by the dopant ions. Thus, structural differences in the alkali-metal-doped $(\text{CH})_x$ systems affect the intrinsic transport properties; however, these may often be masked by the effects of disorder.

B. Temperature and pressure dependence

From previous temperature dependence of conductivity for K-, Rb-, and Cs-doped $(\text{CH})_x$ it is known that neither the fluctuation-induced tunneling model nor the variable-range hopping provide a satisfactory model for the conduction mechanism.⁴ The temperature dependence of conductivity of stretched-oriented $(\text{CH})_x$ indicates improvement in the transport properties, as is evident by the rather small ratio $\rho(250 \text{ K})/\rho(1.2 \text{ K}) \approx 25$ for K-doped $(\text{CH})_x$ (as can be seen in Fig. 3). However, for Na-doped $(\text{CH})_x$ a stronger temperature dependence is observed, resulting in a larger ratio of $\rho(250 \text{ K})/\rho(4.2 \text{ K}) \approx 105$. As mentioned before, the overlap of the wave

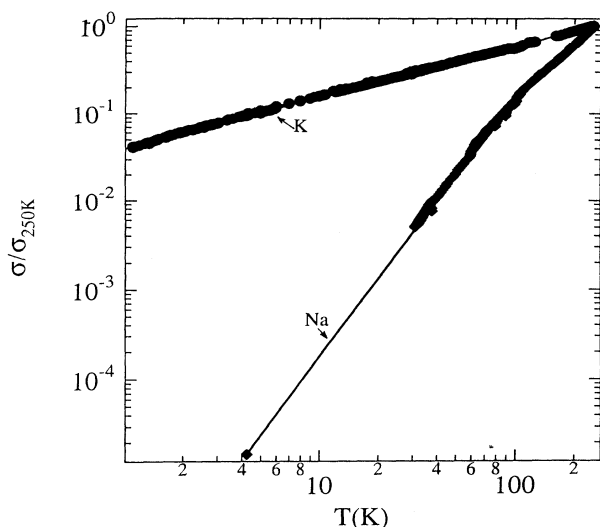


FIG. 3. Normalized conductivity vs temperature for Na- and K-doped $(\text{CH})_x$ in log-log scale.

function of the localized states in K-doped $(\text{CH})_x$ is much higher than that in Na-doped $(\text{CH})_x$ [and possibly the doping-induced disorder is smaller in K-doped $(\text{CH})_x$]. This corresponds to the weaker temperature dependence observed for K-doped $(\text{CH})_x$ as compared to Na-doped $(\text{CH})_x$. The best fits of the conductivity versus temperature (shown in Fig. 3) for these systems follow a power law, $\sigma \propto T^n$, where n is 0.57 and 2.6 for K- and Na-doped $(\text{CH})_x$, respectively. Power-law dependence has been recently observed in polyaniline²⁴ and polypyrrole,²⁵ and has been theoretically predicted for systems at the critical regime near the metal-insulator transition, at which the Fermi level is near the mobility edge.²⁶

A study of the effect of interchain coupling is obtained by measuring the pressure dependence of the conductivity of K-doped $(\text{CH})_x$. The hydrostatic pressure is applied to the sample after the conductivity is stabilized for 5–8 h at the maximum doping level. As is shown in Fig. 4,

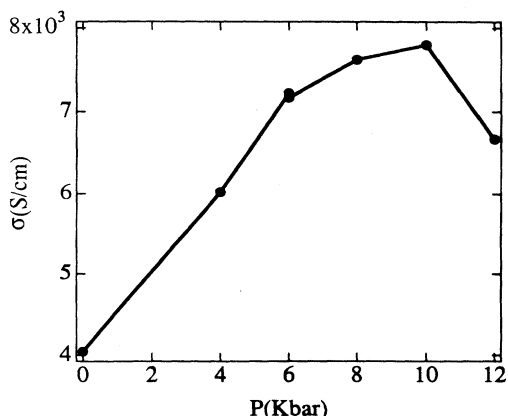


FIG. 4. Conductivity vs pressure for K-doped $(\text{CH})_x$.

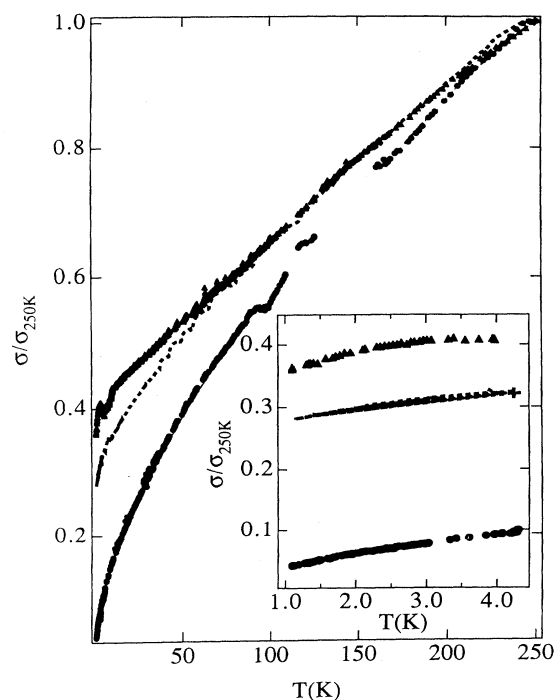


FIG. 5. Normalized conductivity vs temperature for K-doped $(\text{CH})_x$ at ambient pressure, 8 kbar, and 10 kbar; inset shows the nearly temperature independent conductivity below 4.5 K.

the results are qualitatively similar to that of pristine $(\text{CH})_x$.²⁷ At 10 kbar the conductivity increases by a factor of ~ 2 , due to the enhancement in interchain interaction that results in a higher probability of interchain hopping. At pressures above 10 kbar, a decrease in conductivity is observed. The exact reason for this decrease is not well understood; it may be due to the enhanced pinning of charge carriers at high pressures as the counterion columns are squeezed closer to the $(\text{CH})_x$ chains, or creation of structural defects, etc.

The temperature dependence of K-doped $(\text{CH})_x$ at various pressures is shown in Fig. 5. Both the ambient conductivity and its variation with temperature are considerably reduced at high pressures. The ratio of $\rho(250 \text{ K})/\rho(1.2 \text{ K})$ for samples at ambient pressure and 10 kbar are 25 and 2.8, respectively. The weaker temperature dependence at high pressures originates from the enhanced interchain interaction, in agreement with our observations of the difference in the temperature dependence of conductivity in Na- and K-doped $(\text{CH})_x$. The inset in Fig. 5 depicts the results for samples under pressure at the low-temperature regime, below 4 K, where a temperature-independent conductivity is observed, similar to the behavior of disordered metals.

CONCLUSIONS

The *in situ* conductivity measurements of alkali-metal-doped $(\text{CH})_x$ display a strong correlation between the electronic and structural properties. The detailed tem-

poral evolution of the conductivity for different alkali-metal dopants can be understood in terms of the effects of interchain interaction, staging of the intercalated compounds, doping-induced structural disorder, and the rate of diffusion of the alkali ions into the polymer matrix. We find that the difference in the time dependence of the conductivity of K- and Na-doped $(\text{CH})_x$ is related to the rate of ionic diffusion and the resultant structural disorder. Similarly, we find that the variations in the temperature dependence of conductivity and the effects of high pressure in these systems could be understood in terms of the magnitude of interchain coupling. Specifically, the higher conductivity of K-doped $(\text{CH})_x$, as compared to that of Na-doped $(\text{CH})_x$, as well as the weaker temperature dependence is correlated with the greater overlap of the soliton wave functions in K-doped $(\text{CH})_x$. The above observations indicate that by increasing the interchain interaction (achieved by doping with smaller metallic ions, or by applying high pressure) the transport properties of quasi-one-dimensional systems can approach near-metallic behavior.

We find that a slow rate of intercalation is essential for

obtaining high conductivity. At a fast doping rate, obtained either by using more concentrated doping solution or by employing alkali metals with smaller ionic size, higher disorder is created, leading to a reduced conductivity and near elimination of staging transitions.

The temperature dependence of the conductivity follows a power law $\sigma \propto T^n$ similar to the behavior observed recently in polyaniline and polypyrrole, in agreement with the theoretical prediction for systems at the critical regime near the metal-insulator transition, for which the Fermi level is close to the mobility edge.

ACKNOWLEDGMENTS

We want to express our gratitude to Dr. Alan Heeger for important discussions, and to R. H. Stuber and the personnel of the machine shop of the Physics Department at UCSB for the technical help they provided in the construction of our transport laboratory. This work has been funded by a grant from the Electric Power Research Institute (EPRI). Support for K.V. was provided by Neste Oy of Finland.

*Present address: Neste Oy, Corporate R&D, P.O.B. 310, SF-06101, Porvoo, Finland.

¹A. B. Kaiser, *Synth. Met.* **45**, 185 (1991), and references therein.

²Y. Nogami, H. Kaneko, T. Ishiguro, A. Takahashi, J. Tsukamoto, and N. Hoshito, *Solid State Commun.* **76**, 583 (1990).

³D. Moses, A. Feldblum, E. Ehrenfreund, A. J. Heeger, T. C. Chung, and A. G. MacDiarmid, *Phys. Rev. B* **26**, 3361 (1982).

⁴F. Saldi, J. Ghanbaja, J. F. Marêché and D. Billaud, *Solid State Commun.* **78**, 941 (1991).

⁵Y. Nogami, H. Kaneko, H. Ito, T. Ishiguro, T. Sasaki, N. Toyota, A. Takahashi, and T. Tsukamoto, *Phys. Rev. B* **43**, 11 829 (1991).

⁶H. H. S. Javadi, A. Chakraborty, C. Li, N. Theophilou, D. B. Swanson, A. G. MacDiarmid, and A. J. Epstein, *Phys. Rev. B* **43**, 2183 (1991).

⁷K. Akagi, M. Suezaki, H. Shirakawa, H. Kyotani, M. Shimamura, and Y. Tanabe, *Synth. Met.* **28**, D1 (1989).

⁸Y. Cao, P. Smith, and A. J. Heeger, *Polymer* **32**, 1210 (1991).

⁹R. L. Elsenbaumer, P. Delannoy, G. G. Miller, C. E. Forbes, N. S. Murthy, H. Eckhardt, and R. H. Baughman, *Synth. Met.* **16**, 251 (1985).

¹⁰B. François and C. Mathis, *Synth. Met.* **16**, 105 (1986); A. Rudatsikira, R. Nuffer, C. Mathis, and B. François, *ibid.* **20**, 303 (1987).

¹¹G. Thummes, F. Körner, and J. Kötzler, *Solid State Commun.* **67**, 215 (1988).

¹²A. Jayaraman, A. R. Hutson, J. H. McFee, A. S. Coriell, and R. C. Maines, *Rev. Sci. Instrum.* **38**, 44 (1967).

¹³H. Fujiwara, H. Kadomatsu, and K. Tohma, *Rev. Sci. Instrum.* **51**, 1345 (1980).

¹⁴N. Basescu, J. Chiang, S. Rughooputh, T. Kubo, C. Fite, and A. J. Heeger, *Synth. Met.* **28**, D45 (1989).

¹⁵F. Moraes, J. Chen, T.-C. Chung, and A. J. Heeger, *Synth. Met.* **11**, 271 (1985).

¹⁶J. Ghanbaja, J. F. Marêché, E. McRae, and D. Billaud, *Solid State Commun.* **60**, 87 (1986).

¹⁷N. Coustel, P. Bernier, and J. E. Fischer, *Phys. Rev. B* **43**, 3147 (1991).

¹⁸N. S. Murthy, L. W. Shacklette, and R. H. Baughman, *Phys. Rev. B* **41**, 3708 (1990), and references therein.

¹⁹M. Winokur, Y. B. Moon, A. J. Heeger, J. Barker, D. C. Bott, and H. Shirakawa, *Phys. Rev. Lett.* **58**, 2329 (1987); S. Flandrois, C. Hauw, and B. François, *Mol. Cryst. Liq. Cryst.* **117**, 91 (1985).

²⁰N. Coustel, C. Fite, and P. Bernier, *Mater. Sci. Forum* **42**, 143 (1989).

²¹J. E. Fisher and T. E. Thompson, *Phys. Today* **31**, 36 (1978).

²²E. M. Conwell, H. A. Mizes, and S. Jeydev, *Phys. Rev. B* **41**, 5067 (1990), and references therein.

²³E. M. Conwell, H. A. Mizes, and S. Jeydev, *Phys. Rev. B* **40**, 1630 (1990).

²⁴M. Reghu, Y. Cao, D. Moses, and A. J. Heeger, *Phys. Rev. B* **47**, 1758 (1993).

²⁵T. Ishiguro, H. Kaneko, Y. Nogami, H. Ishimoto, H. Nishiyama, J. Tsukamoto, A. Takahashi, M. Yamaura, T. Hagiwara, and K. Sato, *Phys. Rev. Lett.* **69**, 660 (1991).

²⁶A. I. Larkin and D. E. Khmel'nitskii, *Zh. Eksp. Teor. Fiz.* **83**, 1140 (1982) [*Sov. Phys. JETP* **56**, 647 (1982)].

²⁷D. Moses, J. Chen, A. Denenstein, M. Kaveh, T.-C. Chung, A. J. Heeger, A. G. MacDiarmid, and Y.-W. Park, *Solid State Commun.* **40**, 1007 (1981).